Matrix Biology Plus

Long filopodia and tunneling nanotubes define new phenotypes of breast cancer cells in 3D cultures

Marco Franchi [a], **Zoi Piperigkou** [b], **Eirini Riti** [b], **Valentina Masola** [c], **Maurizio Onisto** [c] and **Nikos K. Karamanos** [b]

a - Department for Life Quality Studies, University of Bologna, Rimini, Italy
b - Biochemistry, Biochemical Analysis & Matrix Pathobiology Research Group, Laboratory of Biochemistry, Department of Chemistry, University of Patras, Patras, Greece
c - Department of Biomedical Sciences, University of Padova, Padova, Italy

Correspondence to Marco Franchi: marco.franchi3@unibo.it
https://doi.org/10.1016/j.mbplus.2020.100026

Abstract

Cancer cell invasion into the surrounding extracellular matrix (ECM) takes place when cell-cell junctions are disrupted upon epithelial-to-mesenchymal transition (EMT). Both cancer cell-stroma and cell-cell crosstalk are essential to support the continuous tumor invasion. Cancer cells release microvesicles and exosomes containing bioactive molecules and signal peptides, which are recruited by neighboring cells or carried to distant sites, thus supporting intercellular communication and cargo transfer. Besides this indirect communication mode, cancer cells can develop cytoplasmic intercellular protrusions or tunneling nanotubes (TNTs), which allow the direct communication and molecular exchange between connected distinct cells. Using scanning electron microscopy (SEM) we show for the first time that MDA-MB-231 (high metastatic potential) and shERβ MDA-MB-231 (low metastatic potential) breast cancer cells cultured on fibronectin and collagen type I or 17β-estradiol (E2) develop TNTs and very long flexible filopodia. Interestingly, the less aggressive shERβ MDA-MB-231 cells treated with E2 in 3D collagen matrix showed the highest development of TNTs and filopodia. TNTs were often associated to adhering exosomes and microvesicles surfing from one cell to another, but no filopodia exhibited vesicle-like cytoplasmic structures on their surface. Moreover, E2 affected the expression of matrix macromolecules and cell effectors mostly in the presence of ERβ. Our novel data highlights the significance of matrix substrates and the presence of E2 and ERβ in the formation of cellular protrusion and the production of surface structures, defining novel phenotypes that unravel nodal reports for breast cancer progression.

Introduction

Extracellular matrix (ECM) refers to a three dimensional (3D) structural and functional scaffold of macromolecules that are in a dynamic interplay forming complex networks interacting with cells through specialized cell receptors and matrix mediators [1–3]. ECM components include fibrillar (collagens, elastin and fibronectin) and non-fibrillar biomolecules [proteoglycans/glycosaminoglycans (PGs/GAGs) and glycoproteins], which exert diverse functions maintaining tissue homeostasis and regulating cell phenotypes. Deregulation of matrix composition affects several pathological conditions, including cancer [4–6]. Tumor invasion, which predates metastasis, involves mutual and dynamic interactions between the primary tumor cells and the surrounding stromal microenvironment. Intercellular communication between cancer cells and particularly between cancer and stromal cells plays an important role in tumor progression [7,8]. Cancer cells are able to interact with different peritumor host cells: blood and lymph endothelial cells, immunocytes and macrophages, fibroblasts called peritumoral fibroblasts or cancer-associated fibroblasts (CAFs) and

myofibroblasts [9–11]. Cancer cells stimulate peritumor fibroblasts to produce growth factors, hormones, and cytokines favoring tumor growth and metastasis [12–14]. In particular, cancer cells secreting growth factors, such as transforming growth factor beta (TGFβ), can activate stromal fibroblasts into CAFs, which increase their contractility and expression of CAF markers, including α-SMA and FAP and further stimulating cancer cell migration, invasion and metastasis [15].

Cancer cells, both by special cytoplasmic protrusions called invadopodia, but also from the tip of cytoplasmic extensions, called microvilli, aberrantly generate and disseminate high amounts of cytoplasmic extracellular vesicles inside of peritumor stroma, the smaller exosomes and the larger microvesicles [16–19]. Extracellular vesicles contain bioactive molecules like signal peptides, matrix metalloproteinases (MMPs), syndecans, hyaluronic acid, microRNAs (miRNAs), lipids, and DNA [22]. In particular, exosomal miRNAs act as signaling molecules and seem to promote the formation and activation of CAFs, thus enhancing cancer cell migration, invasion and metastasis by regulating ECM [20]. Moreover, specific miRNAs have been recently emerged as important regulators of breast cancer cell behavior and matrix composition depending on estrogen receptor (ER) status [21,22].

The mechanisms of microvesicle and exosome cell uptake and subcellular fate within recipient cells still remain elusive. A novel physiologic function of filopodia for exosome capture has been recently demonstrated by cell live imaging in human primary fibroblasts, showing that they may act as highways for cell entry of exosomes [23]. In addition to tumor-stromal crosstalk via cytoplasmic vesicles, an alternative means for intercellular communication was also suggested by direct cytoplasmic connections between distant cells. Thin tubular structures connecting single distant cells and allowing direct communication by facilitating the transfer of membrane vesicles were firstly observed in 2004 in cultured rat pheochromocytoma PC12 cells [24]. These bridge-like, F-actin-containing cytoplasmic membrane extensions running straight and not adhering to the culture substratum were named tunneling nanotubes (TNTs) and they show quite different structural features compared to filopodia [25]. They extend up to 100 μm in length indicating that TNT length can be dynamically regulated, with diameters ranging from 50 to 200 nm in neuronal PC12 cells and 180–380 nm in T cells, but even 800 nm in mesothelioma cells [26,27]. The gap-junction in TNT tips has been recently demonstrated suggesting that this intercellular system might act as synapse-like structures playing a role in the long-range transfer of electrical signals [28]. TNTs might not be just passive open conduits but rather are regulated by gating mechanisms.

Different types of TNTs have been found in different cell lines and are characterized by their diversity in terms of morphology and structure [29,30]. In human monocyte-derived macrophages, thick nanotubes (≥0.7 μm) containing microtubules allow traffic of vesicles (endosomes and lysosomes, but also mitochondria) over long distances, while beads and bacteria "surf" using a constitutive flow of the nanotube surface takes place along thin nanotubes (≤0.7 μm) lacking microtubules [31]. TNTs, establishing a direct connection between the cytoplasm of connected cells or in some cases interfacing with gap junctions in plasma membranes, serve as conduits for intercellular shuttling of cellular organelles and other cargo between connected, non-adjacent cells [25,27,32–34]. Sartori-Rupp and co-workers well described TNTs in CAD (mouse catecholaminergic neuronal cell line, Cath.a-differentiated) cells using correlative focused-ion beam scanning electron microscopy (FIB-SEM), scanning electron microscopy (SEM), light- and cryo-electron microscopy approaches to elucidate the structural organization of neuronal TNTs [35]. They found both individual TNTs but also bundle of thin open-ended individual TNTs which contain vesicles and mitochondria and that are held together by threads labeled with anti-N-cadherin antibodies.

Besides the vesicles and mitochondria, also influenza viruses and HIV can spread using TNTs intercellular networks that connect epithelial cells, thus evading immune and antiviral defenses [16,28,36]. Moreover, TNTs were described in different cell types [29], including neurons [37], myeloid cells [38–40], human and murine T cells [40], normal rat kidney cells, rat cardiac myocytes [41] and endothelial progenitor cells [42]. TNTs were also described in different cancer cells like human mesothelioma and lung adenocarcinoma tissues [34], prostate cancer cells [43], breast cancer cells, ovarian cancer cells, pancreatic cancer, human bladder carcinoma cells [44], osteosarcoma and human ovarian adenocarcinoma [45] and colon cancer cells [46]. Recent reports suggest the novel role of TNTs in drug resistance via the intercellular transfer of proteins responsible for causing and/or maintain resistance [47,48]. Even though the morphological characteristics still remain the main criteria for TNTs identification, as no TNT-specific protein marker is known for all TNT types [49,50], only very few groups deeply examined the ultrastructure of TNTs using SEM and transmission electron microscopy (TEM) [16,24,26,28,35,44].

We previously demonstrated the regulatory role of different fibrillar collagen arrays in modifying breast cancer cell shape, inducing epithelial-to-mesenchymal transition (EMT), altering ECM and modulating the formation of extracellular vesicles in breast cancer cells with different ER status [i.e. MCF-7 (ERα-positive) and MDA-MB-231 (ERβ-positive)] [51]. In

this study we analyze the ultrastructure of cytoplasmic protrusions which could be involved in intercellular communications in breast cancer cells with different ERβ status [MDA-MB-231 (ERβ-positive) and shERβ MDA-MB-231 (ERβ-suppressed)] seeded in 3D cultures with different microenvironments (fibronectin or collagen microenvironment), with or without 17β-estradiol (E2) treatment.

Results

Breast cancer cells grown on collagen and fibronectin develop long filopodia and TNTs

We previously demonstrated that ERβ suppression on MDA-MB-231 cells critically affected their morphological mesenchymal characteristics, by reducing their cytoplasmic protrusions and contributing in weakening their aggressive phenotype [52]. In this study, SEM investigation revealed that both MDA-MB-231 and shERβ MDA-MB-231 cells cultivated in 3D cultures on Millipore filters and on filters covered with collagen type I or fibronectin with or without E2 treatment developed cytoplasmic protrusions with different size and diameter. In general, two kinds of cytoplasmic protrusions can be distinguished. The first kind refers to relatively larger (300–500 nm in diameter) curvy cytoplasmic protrusions, conical shaped, 10–80 μm long, which exhibit the morphological aspect of long filopodia, spreading out from the ventral side of cells always adhering to the culture ground or substrate. The second discernment includes the bridge-like ultrafine protrusions 5–40 μm long with a constant diameter of about 50–300 nm, which in some cases reached 900 nm (Fig. 1A, B). They refer to straight intercellular connections, corresponding to TNTs, with a regular cylindrical shape, connecting two distant cells and having no contact with the culture ground/substrate (Fig. 1C, D). Intriguingly, the first kind of protrusions
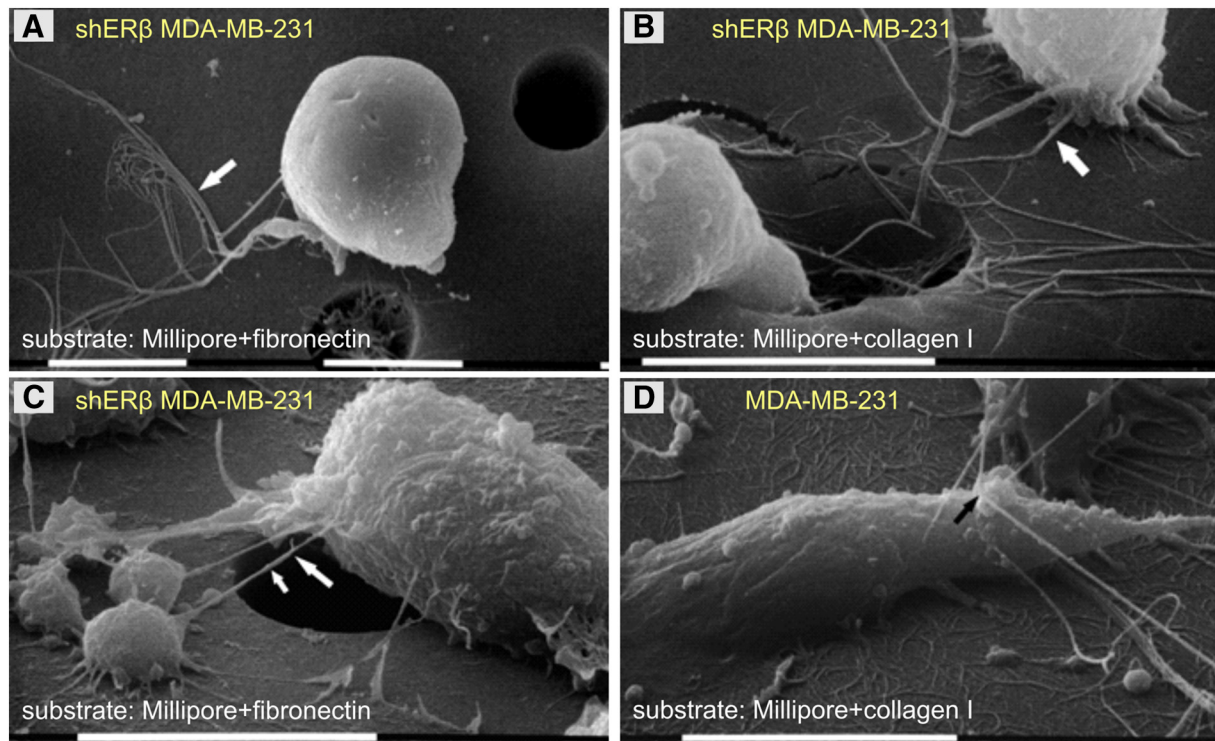

Fig. 1. (A) 3D culture of shERβ MDA-MB-231 cells treated with E2 on Millipore filter covered with fibronectin. A globular cell next to a hole of Millipore filter show long and flexible filopodia (arrow) arising from the ventral side of the cell and spreading out radially in the microenvironment. Scale bar = 10 μm. (B) 3D culture of shERβ MDA-MB-231 cells treated with E2 on Millipore filter covered with collagen. Two cells show long filopodia (arrow) arising from the ventral side of the cells, adhering to the ground and penetrating the Millipore hole partially filled with collagen. Scale bar = 10 μm. (C) 3D culture of shERβ MDA-MB-231 cells treated with E2 on Millipore filter covered with fibronectin. A large cell (on the right) is connected to small globular cells (on the left) by TNTs. The lower result from apposition of two cytoplasmic processes originated from the big and a small cell (large arrow). On this TNT an exosome is detectable (small arrow). Scale bar = 10 μm. (D) 3D culture of MDA-MB-231 cells treated with E2 on Millipore filter covered with collagen. A TNT passes over an elongated and fusiform cell without showing any tight adhesion or fusion with the cytoplasmic membrane (black arrow). Collagen fibrils are visible on the ground. Scale bar = 10 μm.

called filopodia, strongly adhere to the culture ground/substrate and arise from the body of some cells radially spreading out to other cells or also towards the holes of the Millipore filter, sometimes penetrating them (Fig. 1B). Moreover, they showed a smooth surface, with their diameter decreasing form the origin to the peripheral tip. These long flexible filopodia, observed both in MDA-MB-231 and shERβ MDA-MB-231 cells, were in general more developed in 3D collagen matrix cultures treated with E2, and in particular increased and looked longer in shERβ MDA-MB-231 cells where they were longer (60–80 μm) and about ten times higher vs. the other ground cultures.(Fig. 1B).

The narrow protrusions, or TNTs, connecting neighboring cells, were observed in both MDA-MB-231 and shERβ MDA-MB-231 cells, but were more prominent in cultures treated with E2 on Millipore filters covered by collagen type I. They were 5–40 μm long and demonstrated a constant diameter, usually ranging from 50 to 300 nm, but in some cases reaching to 900 nm. It was not unusual to detect round protrusions, emerging from the surface of TNTs, that presumably correspond to microvesicles and smaller exosomes (Figs. 1C, 2B, C and E). TNTs appeared in continuity with the cytoplasmic membrane of two connecting cells, but in some cases, they joined more than one cell and showed only a very tight adhesion to the plasma membrane of the intermediate cells (Fig. 1C). As far as the biogenesis of TNTs is concerned, the ultrastructural observations showed that both cells connected through TNTs developed extended cytoplasmic protrusions towards each other in a definite orientation (Fig. 2A, B and D).

The larger TNTs were distinguishable from long filopodia of similar diameter mainly because they first looked like hanged ropes between and over the cells. Moreover, filopodia always appeared as single, isolated cytoplasmic protrusions, whereas at higher enlargements, TNTs with larger diameter run in interconnected bundles of single TNTs following a slight spiral array (Fig. 2E and F). As we have previously described, the presence of ERβ regulates the morphological characteristics of breast cancer cells determining their aggressive phenotype [62]. In this study, we observed that in all substrates, MDA-MB-231 and shERβ MDA-MB-231 cells displayed differently distributed phenotypes. We confirmed that the cultures of MDA-MB-231 included globular cells and elongated or spindle-like cells but only few polygonal and flattened ones, whereas shERβ MDA-MB-231 cultures showed globular cells and flattened polygonal ones, yet only a few elongated cells (Fig. 1D, 2B and C). Notably, E2 treatment highly affected breast cancer cells by favoring the growth of both long filopodia and TNTs (Fig. 2C and D). Regarding the cytoplasmic surface in all substrates, even if it was not constantly observable in all cells of

each groups, MDA-MB-231 cells showed in general more microvesicles and microvilli (also ten times higher) (Fig. 2A, C and E) when compared to the smoother shERβ MDA-MB-231 cell surfaces (Fig. 2B, D and F).

ERβ regulates the expression of matrix macro-molecules in an E2-independent manner in shERβ MDA-MB-231 cells

The observations on the E2-dependent morphological changes of MDA-MB-231 breast cancer cells before and after ERβ suppression in different matrix substrates, prompted us to investigate the molecular basis of E2 effects on matrix composition of breast cancer cells in order to correlate the E2-mediated effects on matrix composition with the observed changes in cell morphology. By this, we investigated whether the already established effects of ERβ suppression in MDA-MB-231 cells [52] may be reversed by E2. The E2-dependent effects on gene expression of several MMPs, PGs, major EMT markers, cell receptors and signaling molecules in MDA-MB-231 and shERβ MDA-MB-231 cells were evaluated. Notably, our data revealed that E2 affects the expression of specific matrix mediators only in the ERβ-positive MDA-MB-231 breast cancer cell line. More specifically, E2 treatment induced MMP7 mRNA levels (ca 25%), while not affecting MT1-MMP, MMP9, TIMP1 and TIMP2 levels in MDA-MB-231 cells (Fig. 3). On the other hand, E2 increased the mRNA levels of the proteolytic enzymes MT1-MMP, MMP7 and MMP9 in shERβ MDA-MB-231 cells (Fig. 3). Moreover, the E2/ERβ signaling pathway reduced the expression levels of the epithelial marker E-cadherin by 50%, which is in accordance with E2 effects on cell morphology (Fig. 4) and upregulated the expression levels of the mesenchymal marker vimentin; however, E2 effects on EMT markers were less prominent in MDA-MB-231 cells (Fig. 4). As far as the expression of transmembrane PGs is concerned, we observed no substantial changes in the mRNA levels syndecan-1 upon E2 treatment in neither of two breast cancer cell lines. However, E2 increased syndecan-2 mRNA levels in ERβ suppressed cells (Fig. 5A). Moreover, E2-treated MDA-MB-231 cells demonstrated increased glypican-1 levels (Fig. 5B). Notably, the expression of the major syndecan degrading enzyme, heparanase (HPSE), was substantially decreased by the presence of E2 in MDA-MB-231 breast cancer cells, whereas in the absence of ERβ, E2 is not able to affect HPSE mRNA levels (Fig. 5C). E2-treated shERβ MDA-MB-231 cells demonstrated increased levels of the angiogenic VEGFR2, whereas the expression of cell receptors EGFR, IGF-IR and HER2 was slightly decreased. Intriguingly, the mRNA levels of these cellular receptors were not significantly affected in ERβ-positive MDA-MB-231 breast cancer cells (Fig. 6A). Finally, no substantial
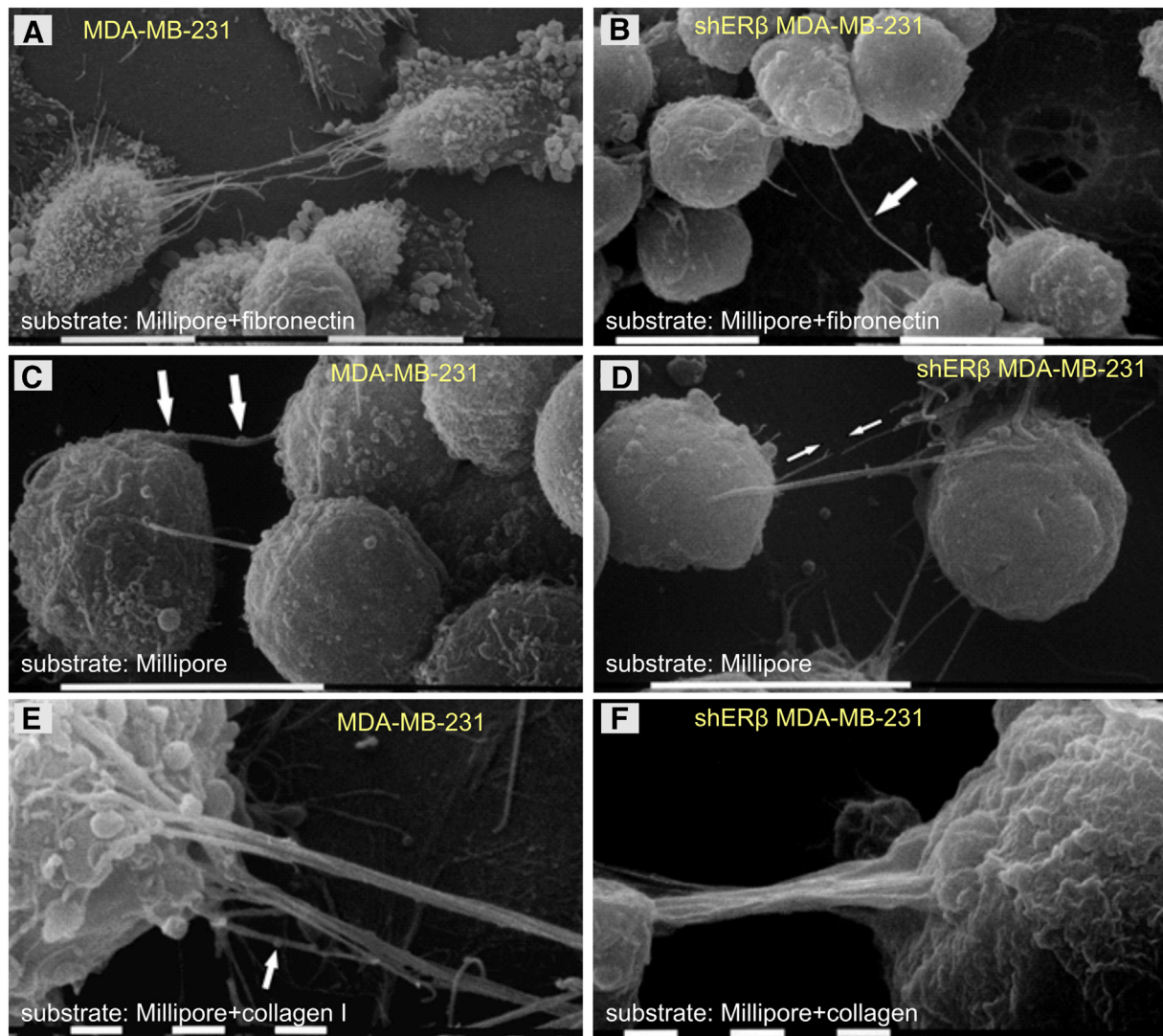
Fig. 2. (A) 3D culture of MDA-MB-231 cells on Millipore filter covered with fibronectin. Ovoidal cells with many microvesicles show straight TNTs and cytoplasmic protrusion presumably forming new TNTs. Scale bar = 10 µm. (B) 3D culture of shERβ MDA-MB-231 cells on Millipore filter covered with fibronectin. Globular cells are connected by thin individual TNTS. Single cytoplasmic protrusions arising from distinct cells suggest the mode of TNTs formation. An exosome is detectable on a TNT (arrow). Scale bar = 10 µm. (C) 3D culture of MDA-MB-231 cells treated with E2 on Millipore filter. Globular cells with microvesicle on the cytoplasmic surface show two distinct individual TNTs connections. On the upper two protrusions (exosomes) are visible (arrows). Scale bar = 10 µm. (D) 3D culture of shERβ MDA-MB-231 cells treated with E2 on Millipore filter. Very smooth globular cells with very few microvesicles and no microvilli are connected by individual straight TNTs. In the upper portion of the pic a TNT seems to form by fusion of two distinct cytoplasmic protrusions (arrows). Scale bar = 10 µm. (E) 3D culture of MDA-MB-231 cells treated with E2 on Millipore filter covered with collagen. Two thick TNTs are composed by single thin individual TNTs branched together in a spiral array. An exosome is attached to a TNT (arrow). Scale bar = 1 µm. (F) 3D culture of shERβ MDA-MB-231 cells treated with E2 on Millipore filter covered with collagen. Two globular cells are connected by a thick TNT that at a higher enlargement shows to be composed by single thin TNTs tight branched together. Scale bar = 1 µm.

changes have been observed in the phosphorylation of Erk1/2 kinases, before and after E2 treatment, in shERβ MDA-MB-231 cells, suggesting that E2 alone is not enough to restore phospho-Erk1/2 in the initial phosphorylation levels, as ERβ presence is crucial for such regulation (Fig. 6B).

Collectively, these data confirmed that ERβ suppression dramatically changes the expression profiles of major matrix mediators, including proteolytic enzymes, PGs, EMT markers, cellular receptors and signaling molecules. Moreover, we demonstrated that the presence of E2 in shERβ MDA-MB-231
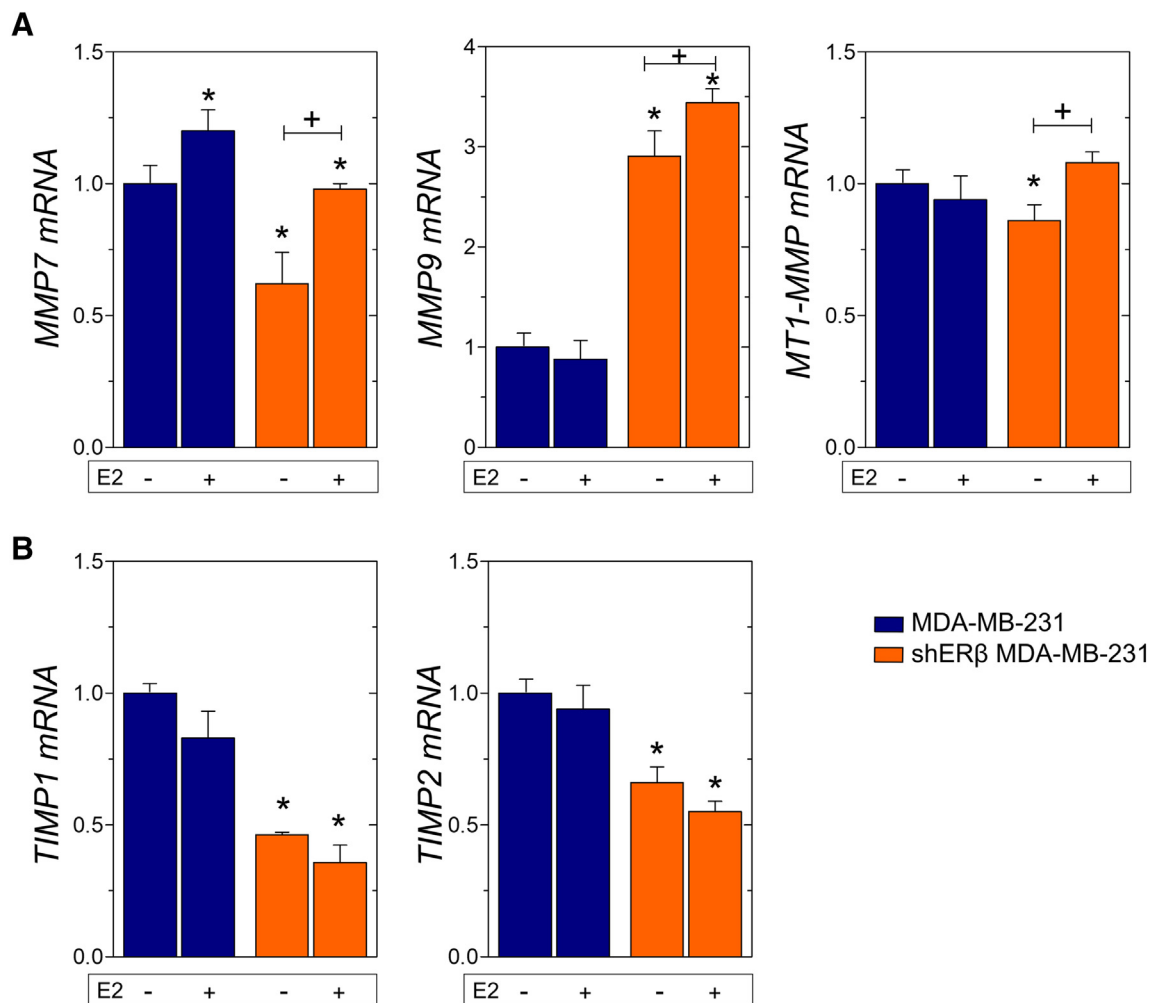
A

B

Fig. 3. Expression of major MMPs in MDA-MB-231 and shERβ MDA-MB-231 cells before and after E2 treatment. Real-time qPCR analysis of (A) MMP7, MMP9, MT1-MMP and (B) TIMP1 and TIMP2 mRNA levels in MDA-MB-231 and shERβ MDA-MB-231 cells, before and after E2 treatment for 16 h. Asterisk (*) indicates statistically significant differences between E2-treated and non-treated MDA-MB-231 cells and between MDA-MB-231 and shERβ MDA-MB-231 cells ($p \leq 0.05$). Cross (+) indicates statistically significant differences between E2-treated and non-treated shERβ MDA-MB-231 cells ($p \leq 0.05$).

cells cannot restore their expression, which in part explains the significantly reduced invasive and metastatic potential of ERβ-suppressed cells.

Discussion

Tumor invasion in neighbor tissues determines the initiation of metastatic process and involves dynamic interactions between the primary tumor cells and the surrounding stromal microenvironment. Cell-cell interactions in tumor stroma involves the shedding of cytoplasmic extravesicles (microvesicles and exosomes) containing bioactive molecules such as signal peptides, MMPs, syndecans, hyaluronan,

miRNAs, lipids, and DNA which are disseminated in the tumor environment and in body fluids of patients with cancer [8,20]. It has also been demonstrated that fibroblast filopodia have a direct mechanical role in exosome capture and represent highways favoring exosomes penetration into the cell [23]. Moreover, cancer cell-cell communication involves thin and straight cytoplasmic intercellular protrusions, called TNTs, which allow a direct bidirectional transfer of proteins, mitochondria, Golgi, and other cytosolic components [44,53]. In this study, we demonstrated and described at the ultrastructural level the presence and morphological aspects of cytoplasmic protrusions, like filopodia and TNTs, which might be involved in exosomes and
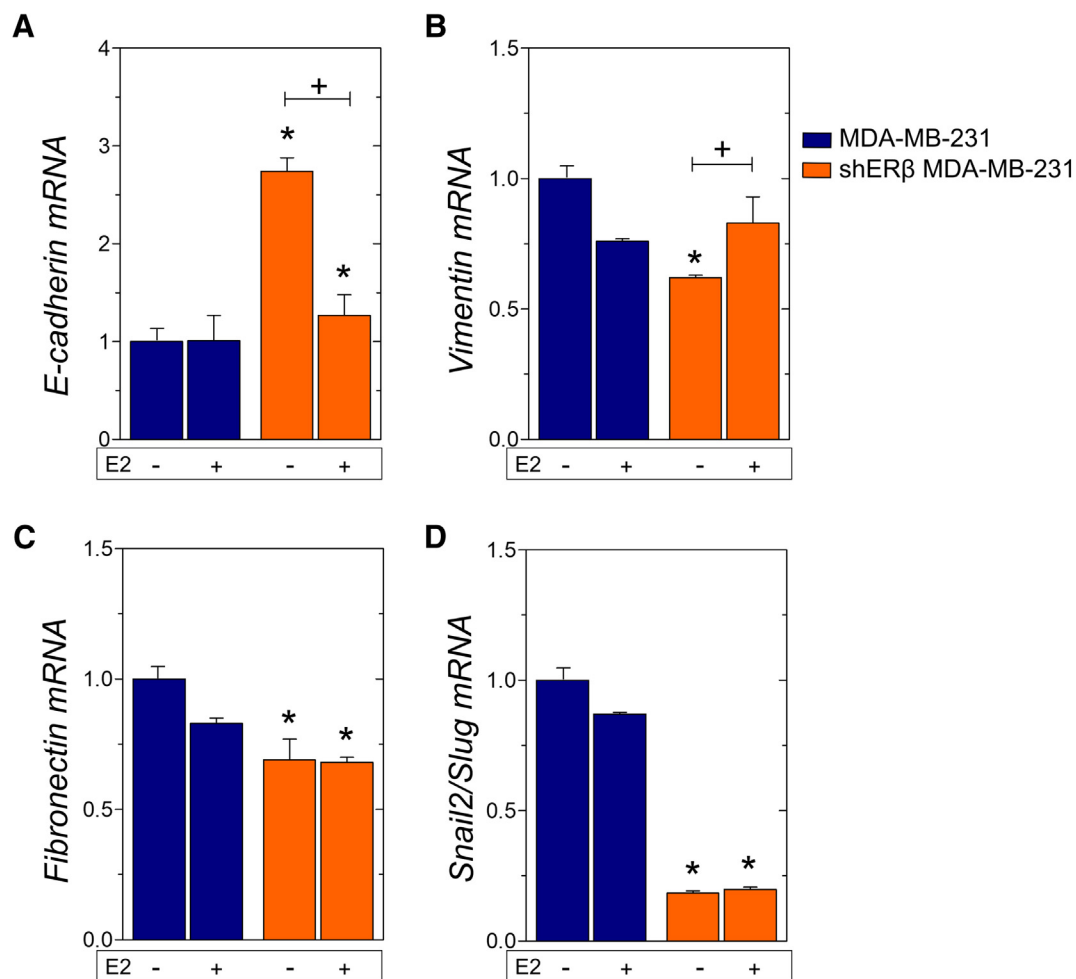
Fig. 4. Effects of E2 on the expression of major EMT markers in MDA-MB-231 and shERβ MDA-MB-231 cells. Real-time qPCR analysis of (A) E-cadherin, (B) vimentin, (C) fibronectin and (D) snail2/slug mRNA levels in MDA-MB-231 and shERβ MDA-MB-231 cells, before and after E2 treatment for 16 h. Asterisk (*) indicates statistically significant differences between MDA-MB-231 and shERβ MDA-MB-231 cells ($p \leq 0.05$). Cross (+) indicates statistically significant differences between E2-treated and non-treated shERβ MDA-MB-231 cells ($p \leq 0.05$).

mitochondria intercellular exchanges through intercellular communications in breast cancer cells [45,46,54].

Although the 2D in vitro cell culture is the most widely used culture system, 3D cultures are more representative to investigate TNTs in cancer [50]. To mimic the in vivo stroma microenvironment of mammary cancer cells we prepared 3D cultures on Millipore filters covered with collagen type I or fibronectin after cell treatment with E2, which is known to promote breast cancer aggressiveness [55]. All samples were analyzed at SEM to investigate how the tumor microenvironment or any particular surface structures could affect the development of TNTs in breast cancer cells with different ERβ status [MDA-MB-231 (ERβ-positive) and shERβ MDA-MB-231 (ERβ-suppressed)]. No specific biomarkers have

been proposed so far to identify TNTs, therefore the morphological investigation still remains the best approach to study these cytoplasmic intercellular connections [50]. Although in all samples we observed both filopodia and thin TNTs intercellular connections, longer and curvy filopodia adhering to the ground and sometimes penetrating into the Millipore holes so as thin TNTs intercellular connections showing exosomes and microvesicles like-structures on their surface were detectable mainly in culture with a collagen substrate after E2 treatment of breast cancer cells in an ERβ-independent manner.

Collagen type I and E2 represent important factors that promote the formation of both TNTs and long filopodia. Previous studies demonstrated that macrophages enhance the formation of TNTs in MCF-7 breast cancer cells and can stimulate the release of
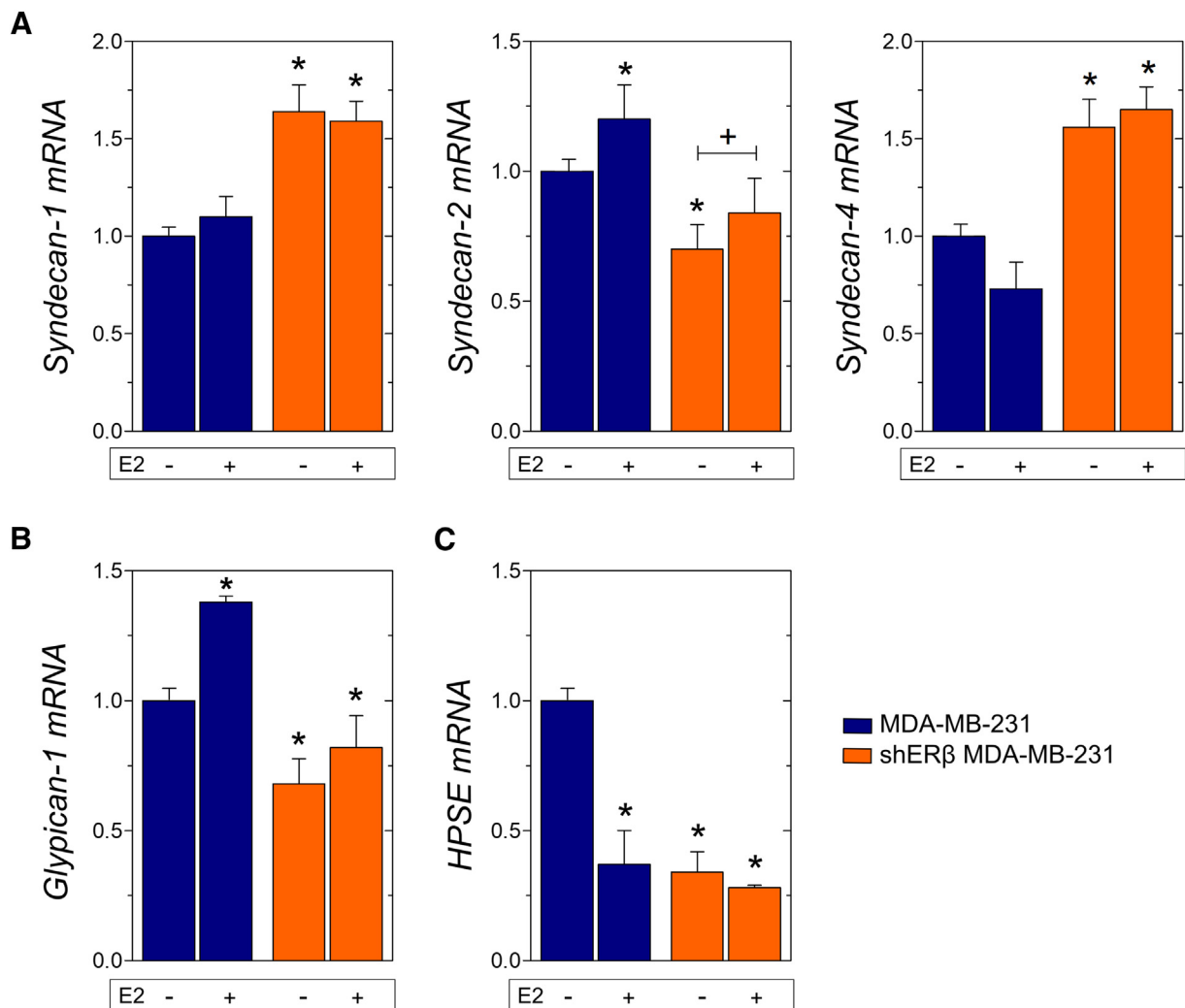
A

B   **C**

■ MDA-MB-231
■ shERβ MDA-MB-231

Fig. 5. Effects of E2 on the expression of cell surface associated PGs in MDA-MB-231 and shERβ MDA-MB-231 cells. Real-time qPCR analysis of (A) syndecan-1, -2, -4, (B) glypican-1 and (C) HPSE mRNA levels in MDA-MB-231 and shERβ MDA-MB-231 cells, before and after E2 treatment for 16 h. Asterisk (*) indicates statistically significant differences between E2-treated and non-treated MDA-MB-231 cells and between MDA-MB-231 and shERβ MDA-MB-231 cells ($p \leq 0.05$). Cross (+) indicates statistically significant differences between E2-treated and non-treated shERβ MDA-MB-231 cells ($p \leq 0.05$).

independently migrating viable cytoplasmic fragments, referred as microplasts, from same cells [56]. Considering our breast cancer model, both filopodia and TNTs were particularly developed in shERβ MDA-MB-231 cells treated with E2 in a collagen network as compared to the MDA-MB-231 cells. All long and flexible filopodia did not show any protrusion which could suggest organelles or vesicles inside the filopodia, whereas TNTs often displayed exosomes like-structures which presumably run from cell to cell. The presence of exosomes and mitochondria inside TNTs has been clearly demonstrated in neuronal cells in a recent report [35]. Besides the single thin and individual TNTs, we demonstrated also TNTs with larger diameter composed of individual thin TNTs branched in a slight spiral array. This particular array may ensure the structural resistance and could favor the movement of exosomes or their exchange through a mechanical shrinkage of single TNTs which occurs when connected cells move away from each other. Notably, it is of great importance that the most developed network of long filopodia and TNTs connections was observed in shERβ MDA-MB-231 breast cancer cells treated with E2, in type I collagen microenvironment.

Our observations under SEM did not confirm the existence of any exosomes or microvesicles on

filopodia surface, thus excluding a possible role of these structures in capturing and favoring exosomes uptake and penetration. Therefore, we suggest that long filopodia might play only sensory and mechanical roles during cell migration. However, filopodia may be equally involved into mechanical and chemical exchanges between tumor cells and the surrounding stroma in vivo, and therefore in tumor invasion and metastasis. This generated the necessity to explain the formation of TNTs as a new cell phenotype related to cancer aggressiveness as suggested by other authors [44,46]. When EMT occurs in cancer cells the cell junctions are disrupted boosting the start of invasion in the surrounding tissue. Cell-cell communication and molecular exchange via traditional cell junctions would be impossible also for an increase of interstitial fluid pressure in tumor microenvironment [57,58]. Therefore, direct intercellular connections like TNTs could be a compensatory support cell survival under stress conditions like local hypoxia and would ensure cell-cell interactions for tumor progression, invasion and metastasis especially in aggressive cells [59].

The next goal of our study was to correlate the morphology related E2 effects with alterations in the molecular level in breast cancer cells with different ERβ status. Our data confirmed that ERβ has a crucial role in the modulation of gene expression of several matrix mediators, including several MMPs, transmembrane PG syndecan-1/-2/-4 and receptor tyrosine kinases in the highly aggressive MDA-MB-231 breast cancer cells. The expression profiles of major ECM macromolecules (MMPs, EMT markers, PGs and cell receptors) were not significantly affected by E2 treatment in shERβ MDA-MB-231 cells. This observation suggests that in the absence of ERβ, E2 is not efficient to restore the expression of critical matrix mediators in control MDA-MB-231 levels.

The present study is the first to describe by SEM the ultrastructure of TNTs with adhering exosomes and microvesicles in breast cancer cells with a different metastatic potential. In addition, we describe for the first time the ultrastructure of large TNTs composed by single TNTs grouped in a spiral array in cancer cells. Ultrastructural investigations about TNTs remains scarce and the mechanisms by which cells communicate with one another are not well understood but further investigations concerning TNTs and intercellular exchanges will help new therapeutic approaches for cancer. Collectively, our novel data pinpointed the significance of ERβ expression in the estrogen-dependent morphological characteristics and invasive potential of MDA-MB-231. These observations open a new area of research to further understand the roles of ECM and improve pharmaceutical targeting of the aggressive breast cancer.

Materials and methods

Chemicals and reagents

Dulbecco's modified Eagle medium (DMEM), fetal bovine serum (FBS), L-glutamine, penicillin, streptomycin were all obtained from Biosera LTD (Courtaboeuf Cedex, France). E2 was supplied by Sigma Chemical Co. (St. Louis, MO, USA). All other chemicals used were of the best commercially available grade.

Cell culture

MDA-MB-231 (high metastatic potential, ERα-negative, ERβ-positive) breast cancer cell line was obtained from the American Type Culture Collection (ATCC) and routinely cultured as monolayers at 37 °C in a humidified atmosphere of 5% (v/v) CO_2 and 95% air. shERβ MDA-MB-231 (ERβ-suppressed cells) were previously described [52]. Breast cancer cells were cultured in DMEM supplemented with 10% (v/v) FBS, 1% L-glutamine and 1% penicillin/streptomycin. Puromycin (0.8 μg/mL) was included in the cultures of shERβ MDA-MB-231 cells. Cells were harvested by trypsinization with 0.05% (w/v) trypsin in PBS containing 0.02% (w/v) Na_2EDTA. All experiments were conducted in serum-free conditions. To better mimic the ECM and the tumor microenvironment both MDA-MB-231 and shERβ MDA-MB-231 breast cancer cells were seeded in 3D cultures prepared on isopore membrane filters, with a pore size of 8.0 μm (Millipore, Milan, Italy), or on similar Millipore filters covered by collagen type I (250 μg/cm^2) or fibronectin (5 μg/cm^2). Similarly, 3D Millipore cultures were performed as described above prior to E2 treatment for 16 h.

SEM imaging

Breast cancer cells seeded in 3D cultures were fixed in a Karnovsky's solution for 30 min at 4 °C. The intact Millipore filters covered by different substrates with adhered cells were rinsed three times with 0.1% cacodylate buffer, dehydrated with increasing concentrations of ethanol and finally dehydrated with hexamethyldisilazane (Sigma-Aldrich, Inc.) for 15 min. All specimens were mounted on appropriate stubs, coated with a 5 nm palladium gold film (Emitech 550 sputter-coater) to be observed under a SEM (Philips 515, Eindhoven, The Netherlands) operating in secondary-electron mode.

RNA isolation and real-time qPCR analysis

Breast cancer cells were grown in serum-containing medium up to 70–80% confluence. Cells

were serum starved for 16 h. Then, E2 (10nM) was added in serum-free culture medium for 16 h. Total RNA was isolated from cells using a NucleoSpin® RNA II Kit (Macherey-Nagel, Duren, Germany). The

amount of isolated RNA was quantified by measuring its absorbance at 260 nm. Total RNA was reverse transcribed using the PrimeScript™ 1st strand cDNA synthesis kit perfect real time (Takara

A

B
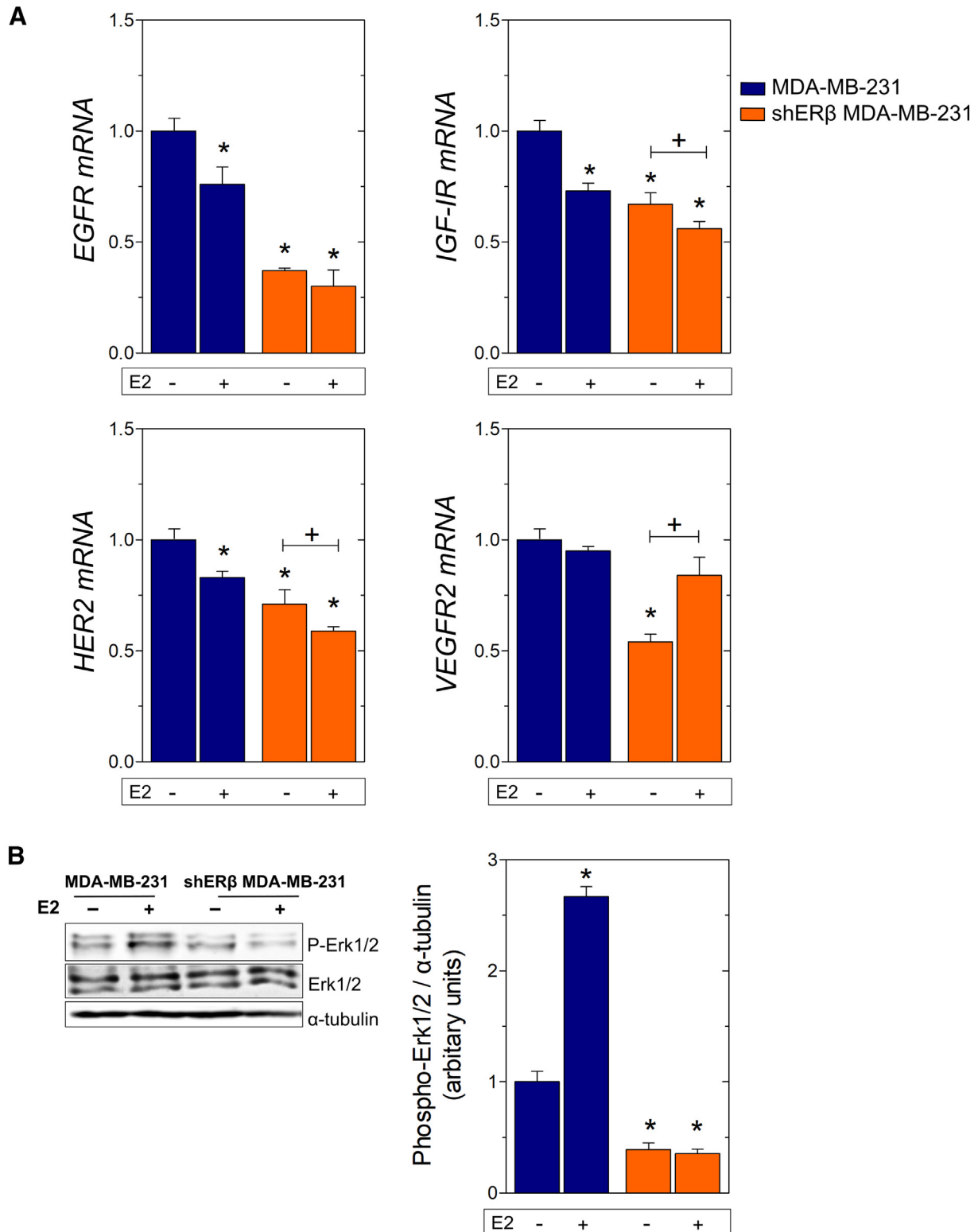
Bio Inc., Japan) and KAPA Taq ReadyMix DNA Polymerase (KAPABIOSYSTEMS). Real-time PCR analysis was conducted in 20 μL reaction mixture, according to the manufacturer's instructions. The amplification was performed utilizing Rotor Gene Q (Qiagen, USA). All reactions were performed in triplicate and a standard curve was always included for each pair of primers for assay validation. In addition, a melting curve analysis was always performed for detecting the SYBR Green-based objective amplicon. To provide quantification, the point of product accumulation in the early logarithmic phase of the amplification plot was defined by assigning a fluorescence threshold above the background, defined as the threshold cycle (Ct) number. Relative expression of different gene transcripts was calculated by the ΔΔCt method. The Ct of any gene of interest was normalized to the Ct of the normalizer (GAPDH). Fold changes (arbitrary units) were determined as $2^{-\Delta\Delta Ct}$. Genes of interest and utilized primers are presented in Supplementary Table 1.

Statistical analysis

Reported values are expressed as mean ± standard deviation (SD) of experiments in triplicate. Statistically significant differences were evaluated using the analysis of variance (ANOVA) test and were considered statistically significant at the level of at least $p \leq 0.05$.

Supplementary data to this article can be found online at https://doi.org/10.1016/j.mbplus.2020.100026.

Funding information

This work has received funding by RFO2018, University of Bologna, Italy.

Author contributions

M.F. performed SEM image analysis and interpretation, had the supervision of the experiments and demonstration of the data. Z.P. performed real-time qPCR analysis, interpretation and demonstration of the data. E.R., V.M. and M.O. prepared the 3D cultures in different substrates. Z.P. and N.K.K. contributed to manuscript writing, experimental design, and editing. All authors reviewed the manuscript.

Declaration of competing interest

The authors declare that they have no known competing financial interests or personal relationships that could have appeared to influence the work reported in this paper.

Fig. 6. Effects of E2 on the expression of cellular receptors and signaling molecules in MDA-MB-231 and shERβ MDA-MB-231 cells. (A) Real-time qPCR analysis of EGFR, IGF-IR, HER2 and VEGFR2 mRNA levels in MDA-MB-231 and shERβ MDA-MB-231 cells, before and after E2 treatment for 16 h. (B) Immunoblots of phospho-Erk1/2, total-Erk1/2 and α-tubulin in MCF-7 and MDA-MB-231 cells in the presence or absence of pre-miR-200b. Asterisk (*) indicates statistically significant between E2-treated and non-treated MDA-MB-231 cells and between MDA-MB-231 and shERβ MDA-MB-231 cells ($p \leq 0.05$). Cross (+) indicates statistically significant differences between E2-treated and non-treated shERβ MDA-MB-231 cells ($p \leq 0.05$).

References

[1] A.D. Theocharis, D. Manou, N.K. Karamanos, The extracellular matrix as a multitasking player in disease, FEBS J. 286 (2019) 2830–2869.

[2] N.K. Karamanos, A.D. Theocharis, T. Neill, R.V. Iozzo, Matrix modeling and remodeling: a biological interplay regulating tissue homeostasis and diseases, Matrix Biol. 75–76 (2019) 1–11.

[3] R.V. Iozzo, M.A. Gubbiotti, Extracellular matrix: the driving force of mammalian diseases, Matrix Biol. 71–72 (2018) 1–9.

[4] A.G. Tavianatou, Z.P. Piperigkou, C. Barbera, R. Beninatto, V. Masola, I. Caon, M. Onisto, M. Franchi, D. Galesso, N.K. Karamanos, Molecular size-dependent specificity of hyaluronan on functional properties, morphology and matrix composition of mammary cancer cells, Matrix Biology Plus, 2019https://doi.org/10.1016/j.mbplus.2019.100008.

[5] K. Kyriakopoulou, E. Kefali, Z. Piperigkou, H. Bassiony, N.K. Karamanos, Advances in targeting epidermal growth factor receptor signaling pathway in mammary cancer, Cell. Signal. 51 (2018) 99–109.

[6] M. Gotte, I. Kovalszky, Extracellular matrix functions in lung cancer, Matrix Biol. 73 (2018) 105–121.

[7] T.T. Chang, D. Thakar, V.M. Weaver, Force-dependent breaching of the basement membrane, Matrix Biol. 57–58 (2017) 178–189.

[8] N. Eiro, L.O. Gonzalez, M. Fraile, S. Cid, J. Schneider, F.J. Vizoso, Breast cancer tumor stroma: cellular components, phenotypic heterogeneity, intercellular communication, prognostic implications and therapeutic opportunities, Cancers (Basel) 11, 2019.

[9] A. Albini, M.B. Sporn, The tumour microenvironment as a target for chemoprevention, Nat. Rev. Cancer 7 (2007) 139–147.

[10] P.J. Barth, C.C. Westhoff, CD34+ fibrocytes: morphology, histogenesis and function, Curr Stem Cell Res Ther 2 (2007) 221–227.

[11] O. De Wever, P. Demetter, M. Mareel, M. Bracke, Stromal myofibroblasts are drivers of invasive cancer growth, Int. J. Cancer 123 (2008) 2229–2238.

[12] C.H. Stuelten, S. DaCosta Byfield, P.R. Arany, T.S. Karpova, W.G. Stetler-Stevenson, A.B. Roberts, Breast cancer cells induce stromal fibroblasts to express MMP-9 via secretion of TNF-alpha and TGF-beta, J. Cell Sci. 118 (2005) 2143–2153.

[13] P. Cirri, P. Chiarugi, Cancer associated fibroblasts: the dark side of the coin, Am. J. Cancer Res. 1 (2011) 482–497.

[14] S.L. Ham, P.S. Thakuri, M. Plaster, J. Li, K.E. Luker, G.D. Luker, H. Tavana, Three-dimensional tumor model mimics stromal - breast cancer cells signaling, Oncotarget 9 (2018) 249–267.

[15] B. Erdogan, D.J. Webb, Cancer-associated fibroblasts modulate growth factor signaling and extracellular matrix remodeling to regulate tumor metastasis, Biochem. Soc. Trans. 45 (2017) 229–236.

[16] A. Kumar, J.H. Kim, P. Ranjan, M.G. Metcalfe, W. Cao, M. Mishina, S. Gangappa, Z. Guo, E.S. Boyden, S. Zaki, I. York, A. Garcia-Sastre, M. Shaw, S. Sambhara, Influenza virus exploits tunneling nanotubes for cell-to-cell spread, Sci. Rep. 7 (2017) 40360.

[17] R.E. McConnell, J.N. Higginbotham, D.A. Shifrin Jr., D.L. Tabb, R.J. Coffey, M.J. Tyska, The enterocyte microvillus is a vesicle-generating organelle, J. Cell Biol. 185 (2009) 1285–1298.

[18] K. Rilla, S. Pasonen-Seppanen, A.J. Deen, V.V. Koistinen, S. Wojciechowski, S. Oikari, R. Karna, G. Bart, K. Torronen, R. H. Tammi, M.I. Tammi, Hyaluronan production enhances shedding of plasma membrane-derived microvesicles, Exp. Cell Res. 319 (2013) 2006–2018.

[19] A. Conigliaro, C. Cicchini, Exosome-mediated signaling in epithelial to mesenchymal transition and tumor progression, J. Clin. Med. 8 (2018).

[20] A.S. Azmi, B. Bao, F.H. Sarkar, Exosomes in cancer development, metastasis, and drug resistance: a comprehensive review, Cancer Metastasis Rev. 32 (2013) 623–642.

[21] Z. Piperigkou, N.K. Karamanos, Estrogen receptor-mediated targeting of the extracellular matrix network in cancer, Semin Cancer Biol https://doi.org/10.1016/j.semcancer.2019.07.006 (2019).

[22] Z. Piperigkou, M. Franchi, M. Gotte, N.K. Karamanos, Estrogen receptor beta as epigenetic mediator of miR-10b and miR-145 in mammary cancer, Matrix Biol. 64 (2017) 94–111.

[23] W. Heusermann, J. Hean, D. Trojer, E. Steib, S. von Bueren, A. Graff-Meyer, C. Genoud, K. Martin, N. Pizzato, J. Voshol, D.V. Morrissey, S.E. Andaloussi, M.J. Wood, N.C. Meisner-Kober, Exosomes surf on filopodia to enter cells at endocytic hot spots, traffic within endosomes, and are targeted to the ER, J. Cell Biol. 213 (2016) 173–184.

[24] A. Rustom, R. Saffrich, I. Markovic, P. Walther, H.H. Gerdes, Nanotubular highways for intercellular organelle transport, Science 303 (2004) 1007–1010.

[25] M. Dupont, S. Souriant, G. Lugo-Villarino, I. Maridonneau-Parini, C. Verollet, Tunneling nanotubes: intimate communication between myeloid cells, Front. Immunol. 9 (2018) 43.

[26] S. Sowinski, C. Jolly, O. Berninghausen, M.A. Purbhoo, A. Chauveau, K. Kohler, S. Oddos, P. Eissmann, F.M. Brodsky, C. Hopkins, B. Onfelt, Q. Sattentau, D.M. Davis, Membrane nanotubes physically connect T cells over long distances presenting a novel route for HIV-1 transmission, Nat. Cell Biol. 10 (2008) 211–219.

[27] J.W. Ady, S. Desir, V. Thayanithy, R.I. Vogel, A.L. Moreira, R. J. Downey, Y. Fong, K. Manova-Todorova, M.A. Moore, E. Lou, Intercellular communication in malignant pleural mesothelioma: properties of tunneling nanotubes, Front. Physiol. 5 (2014) 400.

[28] G. Okafo, L. Prevedel, E. Eugenin, Tunneling nanotubes (TNT) mediate long-range gap junctional communication: implications for HIV cell to cell spread, Sci. Rep. 7 (2017) 16660.

[29] S. Abounit, C. Zurzolo, Wiring through tunneling nanotubes–from electrical signals to organelle transfer, J. Cell Sci. 125 (2012) 1089–1098.

[30] L. Marzo, K. Gousset, C. Zurzolo, Multifaceted roles of tunneling nanotubes in intercellular communication, Front. Physiol. 3 (2012) 72.

[31] B. Onfelt, S. Nedvetzki, R.K. Benninger, M.A. Purbhoo, S. Sowinski, A.N. Hume, M.C. Seabra, M.A. Neil, P.M. French, D.M. Davis, Structurally distinct membrane nanotubes between human macrophages support long-distance vesicular traffic or surfing of bacteria, J. Immunol. 177 (2006) 8476–8483.

[32] H.H. Gerdes, N.V. Bukoreshtliev, J.F. Barroso, Tunneling nanotubes: a new route for the exchange of components between animal cells, FEBS Lett. 581 (2007) 2194–2201.

[33] X. Wang, M.L. Veruki, N.V. Bukoreshtliev, E. Hartveit, H.H. Gerdes, Animal cells connected by nanotubes can be electrically coupled through interposed gap-junction channels, Proc. Natl. Acad. Sci. U. S. A. 107 (2010) 17194–17199.

[34] E. Lou, S. Fujisawa, A. Morozov, A. Barlas, Y. Romin, Y. Dogan, S. Gholami, A.L. Moreira, K. Manova-Todorova, M.A. Moore, Tunneling nanotubes provide a unique conduit for intercellular transfer of cellular contents in human malignant pleural mesothelioma, PLoS One 7 (2012), e33093.

[35] A. Sartori-Rupp, D. Cordero Cervantes, A. Pepe, K. Gousset, E. Delage, S. Corroyer-Dulmont, C. Schmitt, J. Krijnse-Locker, C. Zurzolo, Correlative cryo-electron microscopy reveals the structure of TNTs in neuronal cells, Nat. Commun. 10 (2019) 342.

[36] K.D. Pedro, A.J. Henderson, L.M. Agosto, Mechanisms of HIV-1 cell-to-cell transmission and the establishment of the latent reservoir, Virus Res. 265 (2019) 115–121.

[37] Y. Wang, J. Cui, X. Sun, Y. Zhang, Tunneling-nanotube development in astrocytes depends on p53 activation, Cell Death Differ. 18 (2011) 732–742.

[38] E.A. Eugenin, P.J. Gaskill, J.W. Berman, Tunneling nanotubes (TNT) are induced by HIV-infection of macrophages: a potential mechanism for intercellular HIV trafficking, Cell. Immunol. 254 (2009) 142–148.

[39] K. Hase, S. Kimura, H. Takatsu, M. Ohmae, S. Kawano, H. Kitamura, M. Ito, H. Watarai, C.C. Hazelett, C. Yeaman, H. Ohno, M-Sec promotes membrane nanotube formation by interacting with Ral and the exocyst complex, Nat. Cell Biol. 11 (2009) 1427–1432.

[40] S.C. Watkins, R.D. Salter, Functional connectivity between immune cells mediated by tunneling nanotubules, Immunity 23 (2005) 309–318.

[41] M. Koyanagi, R.P. Brandes, J. Haendeler, A.M. Zeiher, S. Dimmeler, Cell-to-cell connection of endothelial progenitor cells with cardiac myocytes by nanotubes: a novel mechanism for cell fate changes? Circ. Res. 96 (2005) 1039–1041.

[42] K. Yasuda, A. Khandare, L. Burianovskyy, S. Maruyama, F. Zhang, A. Nasjletti, M.S. Goligorsky, Tunneling nanotubes mediate rescue of prematurely senescent endothelial cells by endothelial progenitors: exchange of lysosomal pool, Aging (Albany NY) 3 (2011) 597–608.

[43] A. Kretschmer, F. Zhang, S.P. Somasekharan, C. Tse, L. Leachman, A. Gleave, B. Li, I. Asmaro, T. Huang, L. Kotula, P.H. Sorensen, M.E. Gleave, Stress-induced tunneling nanotubes support treatment adaptation in prostate cancer, Sci. Rep. 9 (2019) 7826.

[44] J. Lu, X. Zheng, F. Li, Y. Yu, Z. Chen, Z. Liu, Z. Wang, H. Xu, W. Yang, Tunneling nanotubes promote intercellular mitochondria transfer followed by increased invasiveness in bladder cancer cells, Oncotarget 8 (2017) 15539–15552.

[45] V. Thayanithy, E.L. Dickson, C. Steer, S. Subramanian, E. Lou, Tumor-stromal cross talk: direct cell-to-cell transfer of oncogenic microRNAs via tunneling nanotubes, Transl. Res. 164 (2014) 359–365.

[46] S. Desir, P. Wong, T. Turbyville, M. Chen, C. Shetty, E. Clark, Y. Zhai, K. Romin, T.K. Manova-Todorova, D.V. Starr, C.J. Nissley, S. Steer, E. Subramanian, Lou, intercellular transfer of oncogenic KRAS via tunneling nanotubes introduces intracellular mutational heterogeneity in colon cancer cells, Cancers (Basel) (2019) 11.

[47] S.V. Ambudkar, Z.E. Sauna, M.M. Gottesman, G. Szakacs, A novel way to spread drug resistance in tumor cells: functional intercellular transfer of P-glycoprotein (ABCB1), Trends Pharmacol. Sci. 26 (2005) 385–387.

[48] N. Lecomte, J.T. Njardarson, P. Nagorny, G. Yang, R. Downey, O. Ouerfelli, M.A. Moore, S.J. Danishefsky, Emergence of potent inhibitors of metastasis in lung cancer via syntheses based on migrastatin, Proc. Natl. Acad. Sci. U. S. A. 108 (2011) 15074–15078.

[49] M.W. Austefjord, H.H. Gerdes, X. Wang, Tunneling nanotubes: diversity in morphology and structure, Commun Integr Biol 7 (2014), e27934.

[50] E.L. Varun Subramaniam Venkatesh, Tunnelling nanotubes, A bridge for heterogeneity in glioblastoma and a new therapeutic target? Cancer Reports e1185 (2019) 1–14.

[51] M. Franchi, V. Masola, G. Bellin, M. Onisto, K.A. Karamanos, Z. Piperigkou, Collagen fiber array of peritumoral stroma influences epithelial-to-mesenchymal transition and invasive potential of mammary cancer cells, J Clin Med 8, 2019.

[52] Z. Piperigkou, P. Bouris, M. Onisto, M. Franchi, D. Kletsas, A. D. Theocharis, N.K. Karamanos, Estrogen receptor beta modulates breast cancer cells functional properties, signaling and expression of matrix molecules, Matrix Biol. 56 (2016) 4–23.

[53] K. Gousset, L. Marzo, P.H. Commere, C. Zurzolo, Myo10 is a key regulator of TNT formation in neuronal cells, J. Cell Sci. 126 (2013) 4424–4435.

[54] J. Pasquier, B.S. Guerrouahen, H. Al Thawadi, P. Ghiabi, M. Maleki, N. Abu-Kaoud, A. Jacob, M. Mirshahi, L. Galas, S. Rafii, F. Le Foll, A. Rafii, Preferential transfer of mitochondria from endothelial to cancer cells through tunneling nanotubes modulates chemoresistance, J. Transl. Med. 11 (2013) 94.

[55] A.I. Tsonis, N. Afratis, C. Gialeli, M.I. Ellina, Z. Piperigkou, S.S. Skandalis, A.D. Theocharis, G.N. Tzanakakis, N.K. Karamanos, Evaluation of the coordinated actions of estrogen receptors with epidermal growth factor receptor and insulin-like growth factor receptor in the expression of cell surface heparan sulfate proteoglycans and cell motility in breast cancer cells, FEBS J. 280 (2013) 2248–2259.

[56] P. Patheja, K. Sahu, Macrophage conditioned medium induced cellular network formation in MCF-7 cells through enhanced tunneling nanotube formation and tunneling nanotube mediated release of viable cytoplasmic fragments, Exp. Cell Res. 355 (2017) 182–193.

[57] L. Lamorte, I. Royal, M. Naujokas, M. Park, Crk adapter proteins promote an epithelial-mesenchymal-like transition and are required for HGF-mediated cell spreading and breakdown of epithelial adherens junctions, Mol. Biol. Cell 13 (2002) 1449–1461.

[58] M.A. Huber, N. Kraut, H. Beug, Molecular requirements for epithelial-mesenchymal transition during tumor progression, Curr. Opin. Cell Biol. 17 (2005) 548–558.

[59] S. Etienne-Manneville, Neighborly relations during collective migration, Curr. Opin. Cell Biol. 30 (2014) 51–59.